ELSEVIER

Hearing Research 174 (2002) 19–31

HEARING RESEARCH

www.elsevier.com/locate/heares

The representation of peripheral neural activity in the middle-latency evoked field of primary auditory cortex in humans[1]

André Rupp [a,*], Stefan Uppenkamp [b], Alexander Gutschalk [a], Roland Beucker [a], Roy D. Patterson [b], Torsten Dau [c], Michael Scherg [a]

[a] *Section of Biomagnetism, Department of Neurology, Universität Heidelberg, 69120 Heidelberg, Germany*
[b] *Centre for the Neural Basis of Hearing, Department of Physiology, University of Cambridge, Downing Street, Cambridge CB2 3EG, UK*
[c] *AG Medizinische Physik, Fachbereich Physik, Universität Oldenburg, 26111 Oldenburg, Germany*

Received 16 April 2002; accepted 23 July 2002

Abstract

Short sweeps with increasing instantaneous frequency (up-chirps) designed to compensate for the propagation delay along the human cochlea enhance the magnitude of wave V of the auditory brainstem responses, while time reversed sweeps (down-chirps) reduce the magnitude of wave V [Dau, T., Wegner, O., Mellert, V., Kollmeier, B., J. Acoust. Soc. Am. 107 (2000) 1530–1540]. This effect is due to synchronisation of frequency channels along the basilar membrane and it indicates that cochlear phase delays are preserved up to the input of the inferior colliculus. The present magnetoencephalography study was designed to investigate the influence of peripheral synchronisation on the activation in primary auditory cortex. Spatio-temporal source analysis of middle-latency auditory evoked fields (MAEFs) elicited by clicks and up- and down-chirps showed that up-chirps elicited significantly larger MAEF responses compared to clicks or down-chirps. Both N19m–P30m magnitude and its latency are influenced by peripheral cross-channel phase effects. Furthermore, deconvolution of the empirical source waveforms with spike probability functions simulated with a cochlear model indicated that the source waves for all stimulus conditions could be explained with the same unit-response function, i.e. a far field recorded cortical response of a very small cell assembly along the medio-lateral axis of Heschl's gyrus that receives input from a small number of excitatory fibres. The conclusion is that (i) phase delays *between* channels in the auditory pathway are preserved up to primary auditory cortex, and (ii) MAEFs can be described by a convolution of a unit-response function with the summary neural activity pattern of the auditory nerve.

Key words: Primary auditory cortex; Auditory image; Magnetoencephalography; Spatio-temporal source modelling; Chirp signal; Auditory evoked field; Cochlear phase delay

1. Introduction

Transient stimuli like clicks are commonly used in electrophysiological research of the human auditory system to elicit synchronised auditory brainstem responses (ABRs) and middle-latency auditory evoked fields (MAEFs). In the cochlea, however, the response to a click is not entirely synchronous; the peak of the

* Corresponding author. Tel.: +49 (6221) 567537; Fax: +49 (6221) 565258.
E-mail address: andre.rupp@urz.uni-heidelberg.de (A. Rupp).

[1] Parts of this study were presented during the 24th Midwinter Research Meeting of the Association for Research in Otolaryngology [Rupp, A., Uppenkamp, S., Gutschalk, A., Dau, T., Patterson, R.D., Scherg, M., 658 (2001) p. 186], St. Petersburg Beach, FL, USA.

Abbreviations: ABR, auditory brainstem response; AIM, auditory image model; AN, auditory nerve; BESA, brain electrical source analysis; BM, basilar membrane; BMM, basilar membrane motion; CAP, compound action potential; GCV, generalised cross-correlation; MAEF/MAEP, middle-latency auditory evoked fields/potentials; MEG, magnetoencephalography; MRI, magnetic resonance image; NAP, neural activity pattern; PAC, primary auditory cortex; PDF, probability density function; α, exponent determining the rate of change of instantaneous frequency in the chirps; m_+, m_-, sign for the phase change in 'Schroeder phase' harmonic complex tones

0378-5955/02/$ – see front matter
PII: S0378-5955(02)00614-7

response occurs several milliseconds later in low frequency channels than it does in high-frequency channels (von Békésy, 1960), because there is an exponential decrease of basilar membrane (BM) stiffness with increasing distance from the base which causes spatial dispersion. In essence, it takes more time for the low-frequency response to reach maximal displacement at the apical end of the cochlea. As a consequence, electrophysiological responses to broadband transients like clicks appear to be largely generated by the synchronised activity of the high-frequency channels on their own.

Several electrophysiological studies in animals and humans indicate that peripheral synchronisation is preserved, at least in the early stages of the auditory pathway. Shore and Nuttall (1985) demonstrated enhanced synchronisation with significantly larger compound action potentials (CAP) in the eighth-nerve fibres of guinea pigs when using up-chirps that were designed to compensate for the spatial dispersion in the cochlea. The analysis of the CAP morphology showed narrower peaks and larger amplitudes for a synchronising up-chirp compared to the time-reversed down-chirp. The authors also showed that lowering the cutoff frequency in high-pass filtered clicks increased CAP latencies. Similar observations were reported by Shore et al. (1987) in ventral cochlear nucleus of the guinea pigs.

Don and Eggermont (1978) measured the human ABR in response to clicks masked by high-pass noise with different cutoff frequencies. This masking technique revealed that the latency to low-frequency stimuli is delayed relative to high frequencies. Don and Eggermont concluded that there must be contributions to the ABR from all regions of the cochlea, although the response is dominated by contributions from the two to three octaves at the basal end.

Dau et al. (2000) and Wegner and Dau (2002) recently demonstrated that up-chirps can affect wave V in the human ABR. The stimulus design is based on the linear cochlear model by de Boer (1980) (Fig. 1). The instantaneous frequency increases from 100 Hz to 10 kHz in about 10 ms (non-linearly), and the chirp is optimised to compensate for the spatial dispersion in the human cochlea. The amplitude of ABR wave V evoked by up-chirps increases, and the latency of the peak relative to stimulus onset is shifted by about 10 ms, when compared to click stimulation or stimulation with time-reversed down-chirps.

In contrast, Wegner et al. (1999) found that chirp direction did not affect the late N100 component of the evoked potentials observed in auditory cortex. They concluded that at the stage where the N100 is generated, neural synchronisation across frequency channels is considerably less important and that neural activity is probably integrated up to about 100 ms. More evidence of temporal integration between inferior colliculus and cortex comes from a recent psychoacoustic study on the perception of short chirps. Uppenkamp et al. (2001) found that down-chirps are perceived as more compact than up-chirps, despite the increased synchronisation produced peripherally by up-chirps and the reduction of synchronisation produced by down-chirps. Computer simulations of the basilar membrane motion (BMM) revealed that clicks and down-chirps exhibit less within-channel ringing than up-chirps, indicating that perception is more determined by within-channel fine structure than between-channel phase differences. This suggests that there is a temporal integration mechanism which removes, or compensates, for phase delays between channels in the auditory pathway before the representation that underlies the perception. This raises the question of whether such a process can be linked to a particular stage in the auditory pathway, and if so, which structure is involved. In this paper, we use MAEFs to investigate the degree to which the phase dispersion in the cochlea is preserved in the the initial cortical representation of transients (clicks and chirps).

Middle-latency auditory evoked potentials (MAEPs) and MAEFs play a major role in the investigation of the primary auditory cortex (PAC). Source analysis of EEG and magnetoencephalography (MEG) data, as well as intracranial studies, indicate that the N19–P30 complex originates from the medial portion of Heschl's gyrus (Scherg et al., 1989, 1990; Gutschalk et al., 1999; Liègeois-Chauvel et al., 1994). Thus, MAEFs provide a non-invasive method for analysing the initial cortical representation of transient sounds.

Several studies indicate that MAEPs are influenced by the frequency content of stimuli. Scherg and Volk (1983) compared wave V ABR and MAEP responses elicited by a click, a low-frequency 'plop' and a 500-Hz tone burst. The peak of wave V, the N19 and the P30 were all significantly delayed in the low-frequency condition (500-Hz tone). Using the high-pass noise masking technique introduced by Don and Eggermont (1978), Scherg et al. (1990) provided further evidence that spatial dispersion along the cochlea has effects up to the level of auditory cortex (the N19–P30 complex). There was a significant shift in the P30 elicited by stimuli restricted to low frequencies. Further evidence for the effects of cochlear dispersion in cortex comes from a recent MEG study by Schneider (2001). By deconvolving transient responses evoked by amplitude modulated tones, he showed that the low-frequency MAEF is shifted by about 8 ms relative to the high-frequency MAEF. These studies support the hypothesis that all regions of the cochlear contribute to the MAEF. However, these studies were carried out using narrow-band signals, so they do not provide evidence concerning

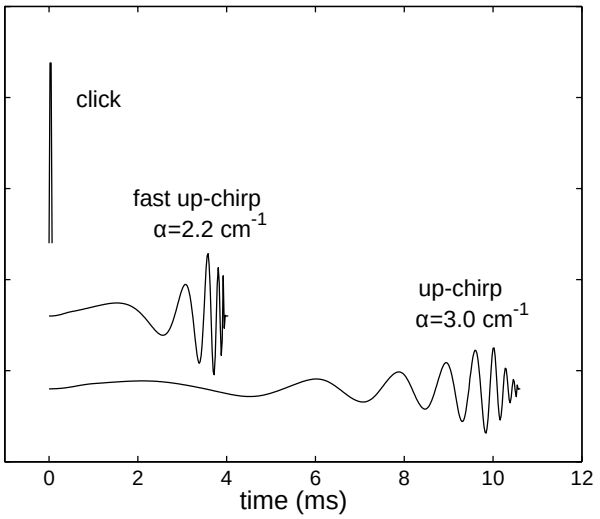

Fig. 1. Waveforms of the stimuli used to evoke MAEF. The solid line shows the sound pressure of the up-chirp with an instantaneous frequency that increases to compensate for the delay along the BM ($\alpha = 3.0$). The slope of the chirp was derived using the linear cochlear model of de Boer (1980). The dotted line shows the sound pressure of a fast chirp with an increased rate of frequency change ($\alpha = 2.2$).

peripheral synchronisation, or the morphology of the MAEF waves elicited by broadband signals.

The objective of the current study was to investigate the role of PAC in the processing of transients, especially the effect of peripheral synchronisation on the activation of PAC and the morphology of the middle latency components. We recorded middle MAEFs elicited by chirp and click stimuli with different rates of change of instantaneous frequency. We anticipated (i) that a higher degree of synchronisation would result in a larger N19m–P30m complex, and (ii) that the latency of the N19m–P30m complex would depend on stimulus type.

We also compared the morphology of the MAEF source waveforms with neural activity patterns (NAPs) that simulate spike probability in the auditory nerve (AN). The analysis indicates that empirical MAEFs can be described as a convolution of a unit response with neural activity in the AN.

2. Auditory evoked fields in response to chirp stimuli

2.1. Methods

2.1.1. Stimuli

Five different stimuli were used: (i) up-chirps with increasing instantaneous frequency (100 Hz to 10 kHz), (ii) down-chirps with decreasing instantaneous frequency (10 kHz to 100 Hz), (iii) fast up-chirps and (v) fast down-chirps with higher rates of frequency change over the same range, and (v) simple clicks. All of the chirp signals were calculated to have flat power spectra (Dau et al., 2000). They were generated using the algorithm published by Dau et al. (2000), which is derived from the 1D linear cochlear model of de Boer (1980). In the model, BM stiffness c as a function of place, x, is given by

$$c(x) = C_0 e^{-\alpha x} \quad (1)$$

with $C_0 = 10^4$ N cm^{-3} and $\alpha = 3$ cm^{-1} for the human cochlea. The mass and damping are assumed to be independent of x. This up-chirp is designed to compensate for the exponential decrease of stiffness and produce maximum excitation all along the cochlear partition simultaneously to synchronise neural firing in the AN. The fast up-chirp and down-chirp were produced by reducing α to 2.2 cm^{-1}. This reduces the stimulus duration to about 4 ms, and so it does not fully compensate for cochlear dispersion. It was hypothesised that fast up- and down-chirps would produce intermediate effects and so provide a check on the manipulation.

Stimuli were generated digitally with a sampling frequency of 44.1 kHz and were balanced for root mean square-values. Digital to analogue-conversion was carried out using a Soundblaster AWE-64 soundcard (Creative Labs Inc.) connected to a PC. The sounds were presented diotically with a home made sound list processor at 40 dB HL via Etymotic Research drivers connected to 90 cm plastic tubes with foam ear-pieces. To minimise electromagnetic distortion 50% of the sounds were delivered with reversed phase. The interstimulus interval was set to 350 ms including randomised jitter of about 50 ms.

2.1.2. MEG recording

Magnetic fields were acquired with a Neuromag-122™ whole head MEG system (Ahonen et al., 1993) inside a magnetically shielded room (IMDECO, Switzerland). Subjects sat in an up-right position and watched a silent movie of their own choice. They were instructed not to pay attention to the sounds. Four coils were attached to the scalp to determine head position under the dewar during the recordings. MEG registration lasted for about 40 min. Horizontal and vertical eye-movements were recorded simultaneously to check for ocular artefacts. Averaging with artefact monitoring was used to increase the signal-to-noise ratio. Single sweeps with an MEG signal exceeding a peak level of 1000 fT, or with a gradient of 800 fT, per sample were rejected. The field was recorded from 50 ms before to 350 ms after stimulus onset. About 1200 single sweeps were gathered for each stimulus con-

dition; when averaged they provided sufficient signal-to-noise ratio to derive stable spatio-temporal source models in all subjects.

2.1.3. Source analysis

Source modelling was carried out using the BESA®2000 software package (MEGIS Software GmbH, Munich, Germany). Prior to source analysis the average data were bandpass filtered offline using a digital, zero-phase-shift Butterworth filter; the pass-band was from 16 to 120 Hz and the skirts outside the band fell away at 6 and 12 dB/octave, respectively. To create an initial multiple source model with an enhanced signal-to-noise ratio, we pooled the data of the click and both down-chirp conditions for each subject. A brain electrical source analysis (BESA)-model with one equivalent dipole in each hemisphere was located near Heschl's gyrus. The final source model was based on the dipole fit covering the N19m–P30m peak-to-peak interval for each individual subject. No further constraints concerning dipole location, orientation or symmetry-condition were applied. In order to compare the different degrees of peripheral synchronisation in all five stimulus conditions with each other, this two-dipole model was held constant and used as a spatial filter for each of the five conditions. The peak latencies and amplitudes of the N19m and P30m were determined in both hemispheres for each subject and each condition, using the source waveforms. Finally, grand average source waveforms were computed for each condition and hemisphere. To determine whether greater synchronisation results in a larger amplitude of the N19m–P30m complex, we compared the N19m–P30m magnitudes of the five different stimulus conditions for each hemisphere separately. To determine whether the MAEF complex was shifted in time by the delays appropriate to the cochlear partition, we compared the latencies of the N19m components. Friedman's non-parametric analysis of variance for repeated measurement (Sprent and Smeeton, 2001) was employed to perform the statistical comparisons (SAS software, version 8). All analyses included pair-wise comparisons with simultaneously adjusted α-errors based on the Holm procedure (Holm, 1979).

2.2. Subjects

Eleven subjects with normal audiometric thresholds and no history of peripheral or central hearing disorder participated in this study (four female, seven male, aged 25–37 years). The subjects were familiar with MEG recording sessions. This experiment was part of a larger research project on temporal processing of the auditory system, which is approved by the local ethics committee.

T1-weighted magnetic resonance images (MRIs) recorded with a Picker 1.5 T scanner were available for 10 out of 11 subjects. There were 180, 1-mm slices in each scan. 2D- and 3D-reconstructions of were computed using BrainVoyager™ (Version 4.0, Brain Innovation B.V., Maastricht, The Netherlands). The centre of the spherical head model for the spatio-temporal analysis was set 5 mm anterior to the posterior commissure.

2.3. Results

The left panel of Fig. 2 shows a subset of 10 original planar gradiometer waveforms recorded in the region of the right temporal plane of subject M.K. in response to the click (grey line), the up-chirp (thick black line) and the down-chirp (thin black line). The waveforms of the sensors showed a clear triphasic MAEF consisting of an N19m followed by a large P30m and an N40m. This complex was followed by a positive deflection in the range 50–70 ms which was not analysed in the present study. The most prominent effect was the enlargement of the N19m–P30m magnitude in the up-chirp condition and a latency shift of these components. The MAEFs for the down-chirps also became broader in the region of the P30m component. This effect was most prominent at sensor CP8C. Further analysis of the data was performed within the framework of equivalent electric dipole sources. Accordingly, the right panel of Fig. 2 shows the results of the multiple source analysis for the same subject. The source waveforms for the equivalent dipole in the right hemisphere reflect the morphology of the raw gradiometer data; that is, the MAEF evoked by the up-chirp exhibits the largest response and it is shifted by about 10 ms relative to the MAEF of the click. In contrast, down-chirps resulted in a broader N19m–P30m with reduced magnitude compared to the click. Fig. 3 shows axial, coronal and sagittal 3D-MRI sections of the same subject. Overlaying the equivalent-dipole solution on the anatomical images showed that the sources were localised at or near the medial portion of Heschl's gyrus. Thus, the location, orientation and latency of the equivalent dipoles indicated that the source activity was in PAC.

For all 11 subjects, it was possible to fit a stable spatio-temporal BESA model with one equivalent dipole in each hemisphere simultaneously to all of the gradiometer data. The grand average source waveforms of the equivalent dipoles in the left (black) and right (grey) hemisphere are shown in the left panel of Fig. 4. The transient MAEF responses exhibited clear N19m–P30m–N40m source components similar to the morphology of the raw sensor waveforms recorded over the temporal lobe of subject M.K. (Fig. 2). The activation patterns of the left and right sources were highly similar in all conditions. As in the single subject data,

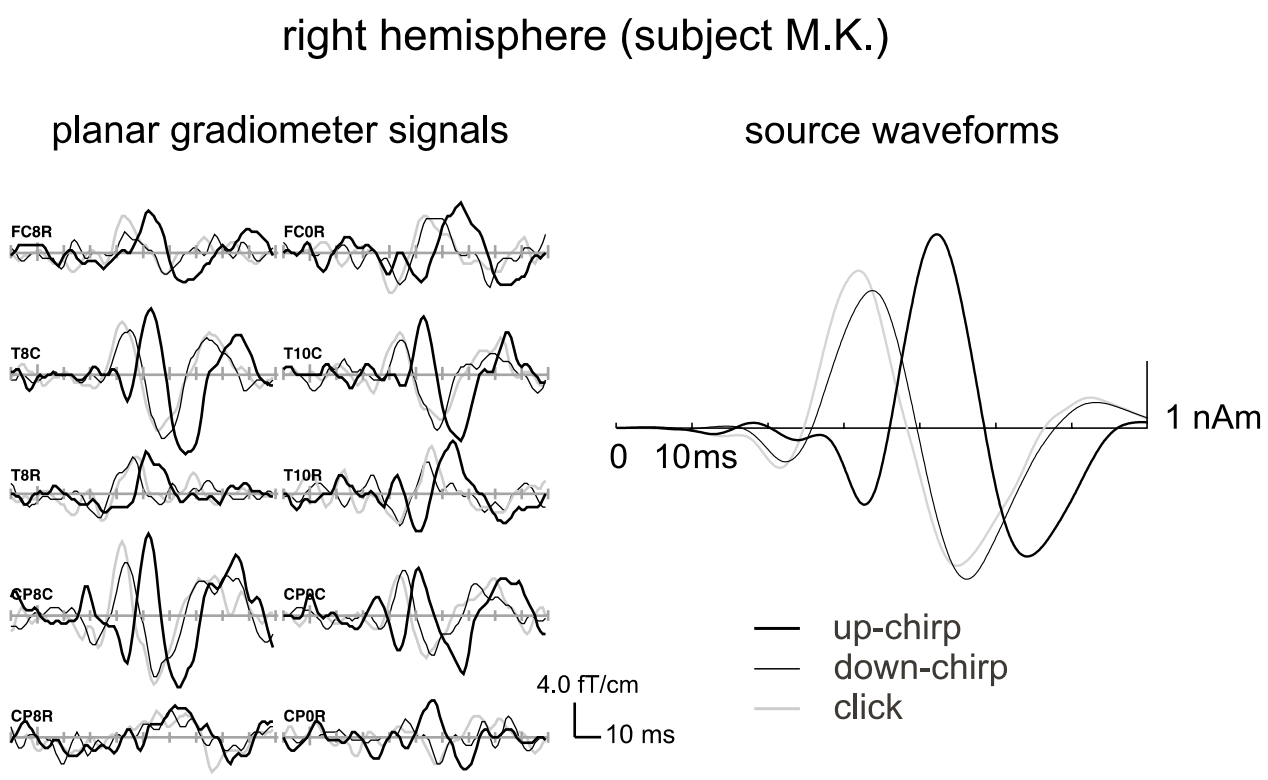

Fig. 2. Left panel: A subset of the original auditory evoked fields of subject M.K. recorded over the right temporal lobe. The planar gradiometer signals show the latitudinal and longitudinal derivatives. Comparison of the sensor waveforms shows the influence of peripheral synchronisation in single-subject data. Most sensor data showed an enlargement of the N19m–P30m magnitude in the up-chirp condition as well as a delayed MAEF response of about 10 ms. The data at CP8C show that the width of the early MAEF response is narrower in the up-chirp condition compared to the down-chirp condition. Right panel: Source waveforms of the equivalent dipole of the right hemisphere derived from a spatio-temporal BESA analysis with one equivalent dipole in each hemisphere. The morphology of the source waveforms is similar to the gradiometer data shown on the left.

the response to the up-chirp is shifted by about 10 ms and the magnitude of the triphasic waves is larger than that for the click response (Fig. 4a). The fast chirps (Fig. 4b) did not produce responses with magnitudes and latencies of the N19m–P30m complex much different from that of the click. The most prominent effect was a time shift in the fast up-chirp response of about 4 ms.

As would be expected from Fig. 4a,b, the Friedman non-parametric analyses of variance indicated highly significant overall differences in the magnitudes between the conditions for both hemispheres (left hemisphere:

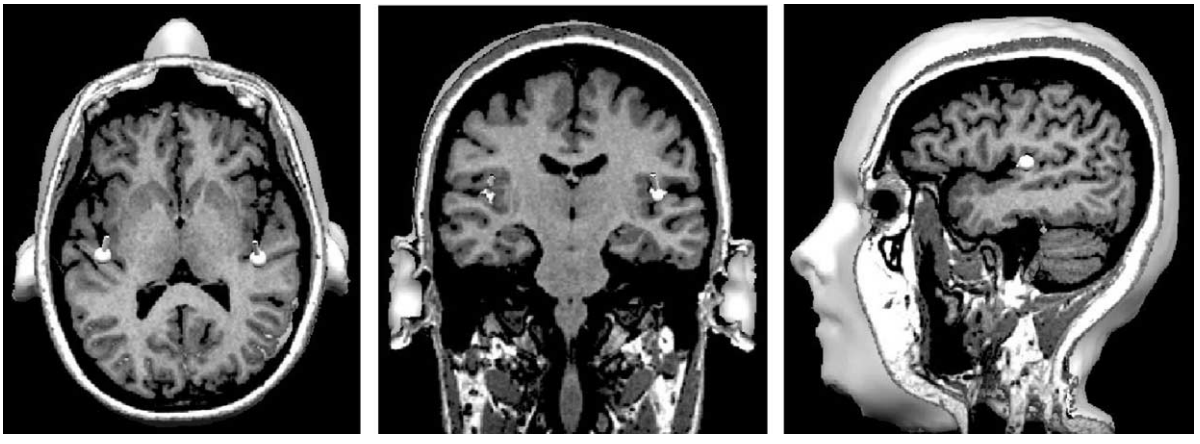

Fig. 3. T1-weighted images for subject M.K. in axial, coronal and sagittal section to illustrate the location of the equivalent dipoles in left and right auditory cortex.

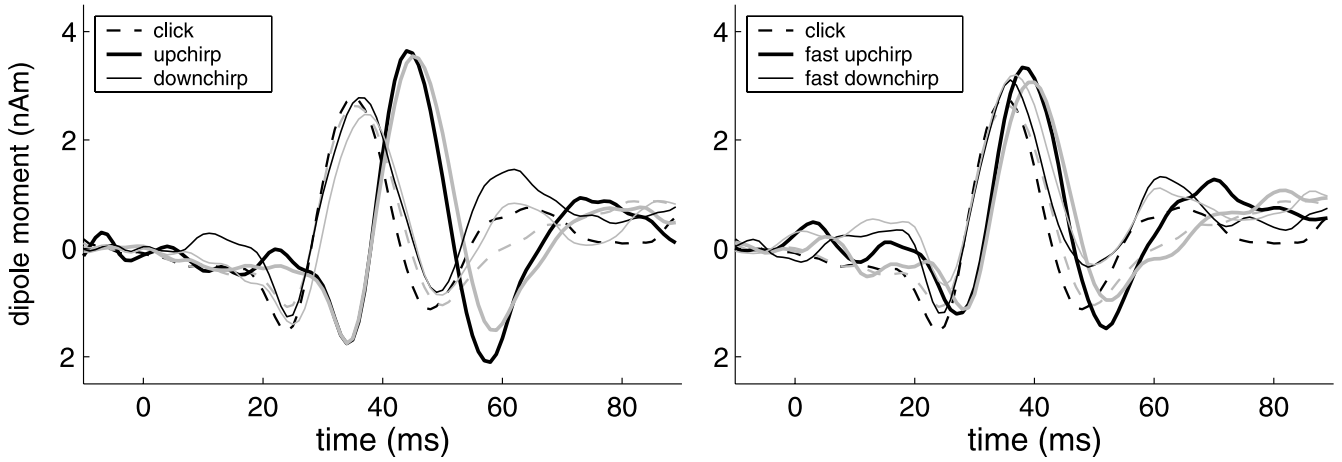

Fig. 4. (a) Grand average MAEFs evoked by clicks, and up-chirps ($\alpha = 3.0$). The thin and thick lines indicate the source waveforms for the left and right hemisphere, respectively. The MAEF response is delayed about 10 ms in the up-chirp condition compared to the click and down-chirp conditions. The enhanced magnitude indicates the influence of peripheral synchronisation on cortical activation. (b) Source waveforms of the fast up- and down-chirps versus the click. The increase of instantaneous frequency rate results in a reduction of the latency difference and amplitude enhancement compared to the up-chirp.

$F = 16.07$, $P < 0.01$; right hemisphere: $F = 27.15$, $P < 0.001$), and in the latencies (left hemisphere: $F = 35.86$, $P < 0.001$; right hemisphere: $F = 36.64$, $P < 0.001$). Table 1 contains the output of the elementwise paired comparisons for the magnitude and latency data. The output of the Holm procedure indicates that the up-chirp enhanced the MAEF magnitude over that produce by the click and the down-chirps in both hemispheres. The down-chirp produced the smallest response of all the stimuli. The magnitude of the click response did not differ significantly from the magnitude of either down-chirp.

Results

The statistical analysis of the P30m latencies showed the expected pattern; elementwise tests indicated that the up-chirp evoked the largest delay in both hemispheres, and that it differed significantly from the latency in all other conditions. As indicated in the grand average waveforms, the fast up-chirp exhibited a smaller shift. The MAEF complex elicited by this chirp was, however, delayed relative to the click by the expected amount. In addition, the analysis of the right hemisphere showed a latency difference for fast up- and down-chirps. The comparison of the magnitude data revealed no significant difference between the click and the up- and down-chirps.

Finally, the morphology of the source waveforms was analysed by comparing the peak-to-peak distances of the N19m and P30m components. A Friedman test indicated an overall difference in the left hemisphere data ($F = 12.15$, $P < 0.05$), whereas the right hemisphere data were not significant ($F = 6.69$, n.s.). However, additional pairwise comparisons revealed a significantly larger peak-to-peak distance for the MAEF evoked by the down-chirp when compared to the MAEF of the up-chirp, in both hemispheres (Table 1c). All other pairwise tests failed to reach the α-adjusted level of significance.

2.4. Discussion

The current experiment was performed to investigate activation patterns in PAC evoked by stimuli that produce varying degrees of neural synchronisation in the peripheral AN. The temporal spread of activation in the AN was manipulated using chirps in which the instantaneous frequency went up or down at one of two rates. Dau et al. (2000) demonstrated that chirp signals with increasing instantaneous frequency that compensate for cochlear phase delays can enhance wave V of the ABR. But there was no significant influence on the N100 component of the AEP (Wegner et al., 1999). Based on these observations, the present experiment was designed to investigate temporal integration at the level of primary cortex using the MAEF.

Spatio-temporal source analysis of the MEG data revealed that, in all 11 subjects, the N19m and P30m represented the first significant deflection of the transient MAEF complex. The equivalent dipoles of the BESA model projected close to the medial portion of Heschl's gyrus. This position is in accordance with earlier auditory evoked magnetic field data (Gutschalk et al., 1999; Rupp et al., 2000) and intracranial data (Liègeois-Chauvel et al., 1994). It suggests that the MAEF components in the present study were generated in PAC. Analysis of the N19m–P30m magnitudes and latencies revealed very similar activation patterns in both hemispheres. These differences in latency and amplitude parallel the findings for the ABR wave V data of Dau et al. (2000). Thus, our data support the hypothesis that neurones along the whole length of the

Table 1
Results of the non-parametric Friedman analysis of variance of the N19m–P30m magnitude (a), the N19m-latency data (b) and the N19m–P30m peak-to-peak distance including pairwise tests with adjusted error levels (c)

PAIR		P	adj $\alpha < 0.05$	adj $\alpha < 0.10$
(a) Magnitude data. Elementwise P-values and simultaneous decisions for $\alpha = 0.05$ and 0.10 based on the Holm procedure:				
Left hemisphere:				
up-chirp	down-chirp	0.001143	1	1
click	up-chirp	0.000977	1	1
up-chirp	fast down-chirp	0.026097	0	0
click	fast up-chirp	0.137658	0	0
up-chirp	fast up-chirp	0.137658	0	0
down-chirp	fast up-chirp	0.137658	0	0
fast up-chirp	fast down-chirp	0.137658	0	0
click	down-chirp	0.391097	0	0
down-chirp	fast down-chirp	0.391097	0	0
click	fast down-chirp	0.778725	0	0
Right hemisphere:				
click	up-chirp	0.000977	1	1
up-chirp	down-chirp	0.000977	1	1
up-chirp	fast up-chirp	0.000977	1	1
up-chirp	fast down-chirp	0.000977	1	1
fast up-chirp	fast down-chirp	0.001143	1	1
down-chirp	fast up-chirp	0.051942	0	0
click	fast up-chirp	0.137658	0	0
click	down-chirp	0.778725	0	0
click	fast down-chirp	0.778725	0	0
down-chirp	fast down-chirp	0.778725	0	0
(b) Analysis of N19m latencies with elementwise P-values and simultaneous decisions for $\alpha = 0.05$ and 0.10 based on the Holm procedure:				
Left hemisphere:				
click	up-chirp	0.000977	1	1
click	fast up-chirp	0.000977	1	1
up-chirp	down-chirp	0.000977	1	1
up-chirp	fast up-chirp	0.000977	1	1
up-chirp	fast down-chirp	0.000977	1	1
down-chirp	fast up-chirp	0.000977	1	1
fast up-chirp	fast down-chirp	0.000977	1	1
click	down-chirp	0.166890	0	0
click	fast down-chirp	0.440522	0	0
down-chirp	fast down-chirp	0.505852	0	0
Right hemisphere:				
click	up-chirp	0.000977	1	1
click	fast up-chirp	0.000977	1	1
up-chirp	down-chirp	0.000977	1	1
up-chirp	fast up-chirp	0.000977	1	1
up-chirp	fast down-chirp	0.000977	1	1
down-chirp	fast up-chirp	0.000977	1	1
fast up-chirp	fast down-chirp	0.000977	1	1
click	fast down-chirp	0.053098	0	0
click	down-chirp	0.095906	0	0
down-chirp	fast down-chirp	0.440522	0	0
(c) Analysis of the MAEF complex width as revealed by the N19m–P30m peak-to-peak distance:				
Left hemisphere:				
up-chirp	down-chirp	0.000002	1	1
up-chirp	fast up-chirp	0.025112	0	0
click	down-chirp	0.051942	0	0
click	up-chirp	0.095906	0	0
up-chirp	fast down-chirp	0.095906	0	0
down-chirp	fast down-chirp	0.095906	0	0
down-chirp	fast up-chirp	0.221235	0	0
click	fast down-chirp	0.276727	0	0
click	fast up-chirp	0.340893	0	0
fast up-chirp	fast down-chirp	0.552739	0	0

Table 1 (*Continued*).

PAIR		*P*	adj $\alpha < 0.05$	adj $\alpha < 0.10$
Right hemisphere:				
up-chirp	down-chirp	0.003910	1	1
down-chirp	fast down-chirp	0.051942	0	0
click	down-chirp	0.166890	0	0
down-chirp	fast up-chirp	0.221235	0	0
click	up-chirp	0.276727	0	0
up-chirp	fast up-chirp	0.276727	0	0
click	fast up-chirp	0.724350	0	0
click	fast down-chirp	0.755967	0	0
up-chirp	fast down-chirp	0.755967	0	0
fast up-chirp	fast down-chirp	0.778725	0	0

cochlear partition contribute to the activation in PAC. The up-chirps constructed to compensate for the spatial dispersion of the travelling wave produced the largest response. Moreover, the MAEF was delayed by about 10 ms relative to the click response. These MAEF data are compatible with the CAP data of Shore and Nuttall (1985). The peak-to-peak distance in the N19m–P30m was much less for the up-chirp than the down-chirp. This broadening in the response to the down-chirp probably reflects the increase in temporal dispersion produced in the cochlea by the down-chirp.

Thus, the latency, amplitude and morphology of the MAEF waveforms all show that between-channel phase differences are still present in the response of PAC. This indicates that there is little, if any, temporal integration for isolated clicks and chirps prior to PAC in the path generates MAEF.

3. Deconvolution of a unit response

Comparison of the source waveforms in Fig. 4 suggests that it is not just the latency and magnitude of the MAEF that are dependent on the degree of peripheral synchronisation; the response evoked by the down-chirp is generally broader than that evoked by the up-chirp. A higher degree of synchronisation results in larger, narrower MAEF peaks. This suggests (i) that there is little temporal integration in the MAEF path up to PAC, and (ii) that the MAEFs might be described as the superposition of unit responses elicited in different tonotopic channels of the auditory system. A simulation was performed to investigate these hypotheses.

Given the cochleotopic organisation of PAC (Webster, 1992) and the CAP data of Shore and Nuttall (1985), we assume that there is no cancellation of the fields produced by individual afferent auditory channels, and that the source waveforms recorded in MEG can be described as the convolution of a neural unit response in auditory cortex with a spike probability function that reflects the sum of peripheral excitation across channels in the AN; that is,

$$MAEF = \textit{peripheral spike probability function} \times \textit{neural unit response} \quad (2)$$

The details of this formulation are presented in Section 3.1. Since single channel unit responses cannot be observed in far field recordings, Eq. 2 cannot be used directly. It is possible, however, to invert the problem and estimate the unit response, or kernel function, which is thought to represent the cortical activation elicited by a small number of afferent fibres in Heschl's gyrus in response to a transient. The fibres might be, for example, a narrow cortical patch along the medio-lateral axis of Heschl's gyrus. This unit response pattern can be derived by deconvolution of the source waveform with summary NAP in the auditory nerve. To test whether such a model could account for the empirical data, we simulated the activity in the AN with a computational model. The deconvolution was computed for each stimulus condition separately and the resulting unit responses were then compared.

3.1. Simulated NAPs from the Auditory Image Model (AIM)

The AIM (Patterson et al., 1992, 1995) is a time-domain model developed to simulate the fine-grain spectro-temporal information in the AN. The 'physiological route' in AIM was employed to simulate peripheral neural activation. The first stage of this model consists of a 1D, transmission-line filterbank that simulates cochlear hydrodynamics (Giguère and Woodland, 1994). The output of this stage simulates BMM, which is then converted into the NAP using a simple hair-cell model (Meddis, 1988). There was one hair-cell simulator for each channel of the filterbank. The filterbank had 500

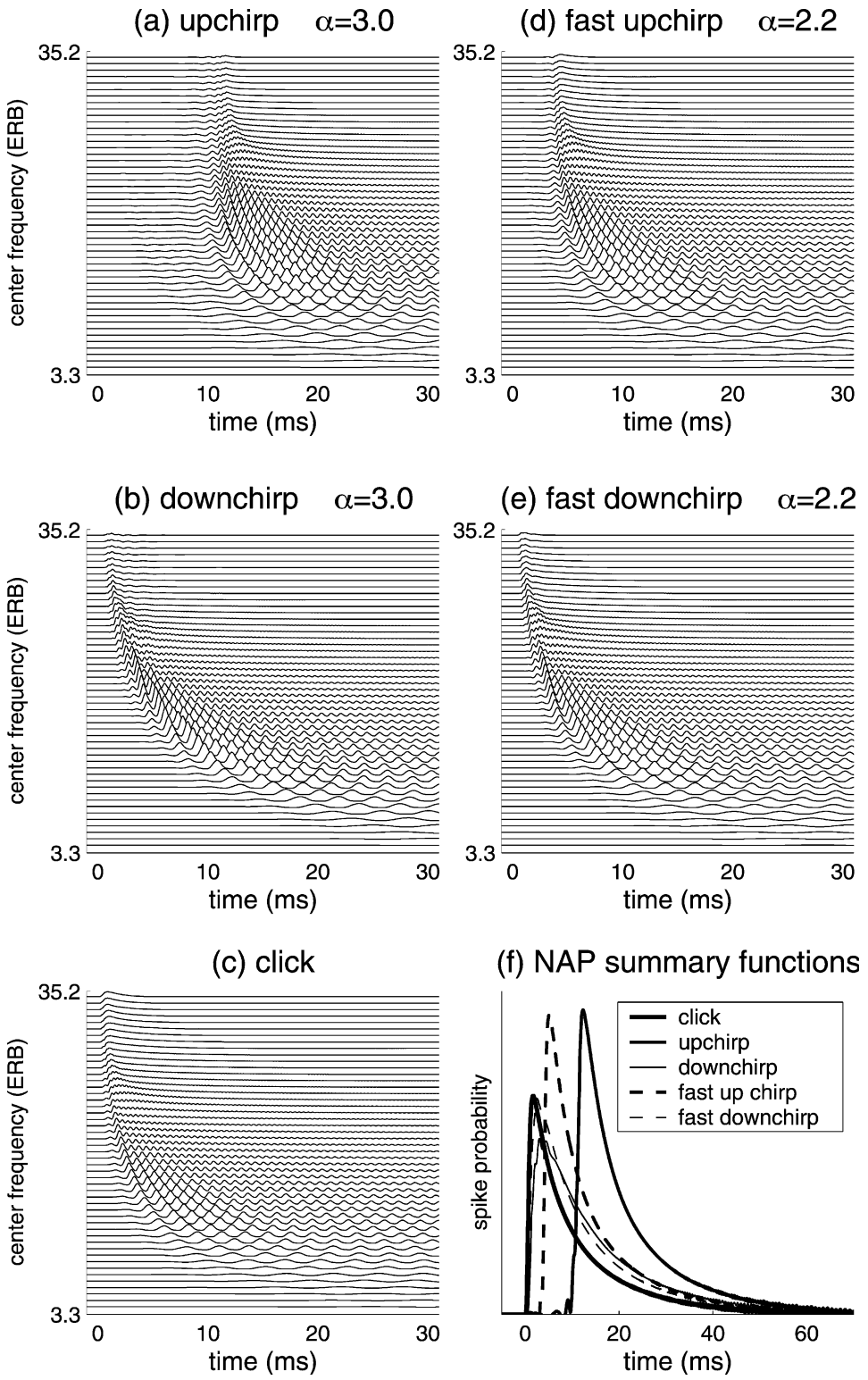

Fig. 5. (a–e) Computer simulations of NAPs based on a 1D, non-linear, transmission-line filterbank. The simulations show the excitation patterns in 50 out of 500 channels. They reveal the ringing of the individual auditory filters. The pattern for the up-chirp (a) is delayed by about 10 ms relative to the pattern for the click (c) and the down-chirp (b); there is also alignment of the point of maximal excitation across frequency channels. Time reversal of the up-chirp leads to a remarkable spread of excitation between channels. (f) The thick solid lines were computed by averaging the activation of all channels of (a) to (e). These curves represent the spike PDFs of the AN.

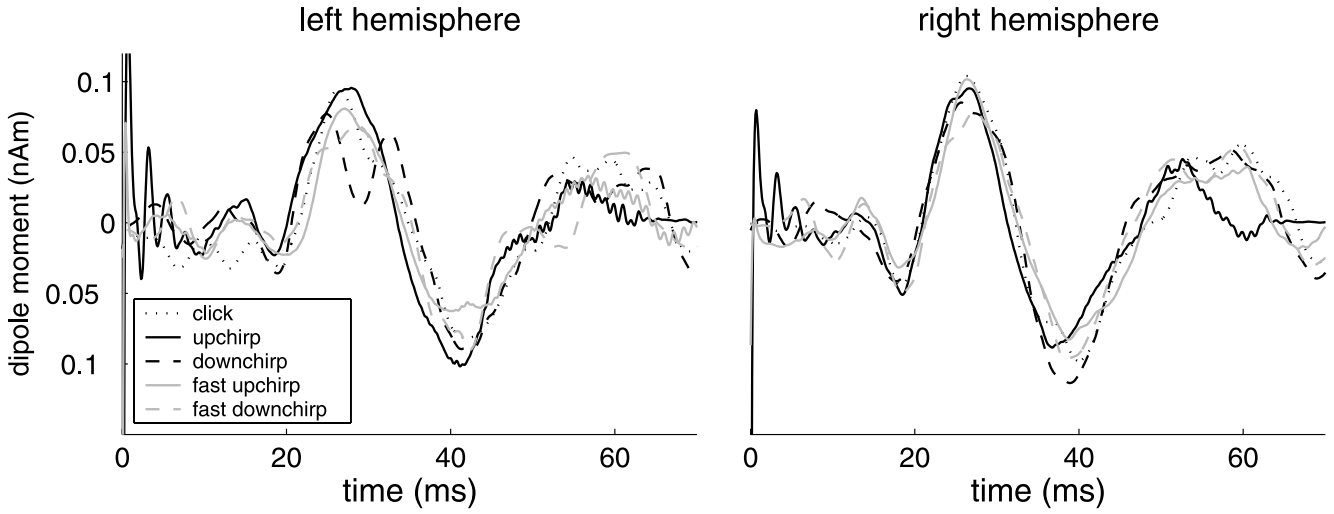

Fig. 6. Deconvolved unit-responses of subject M.K. Deconvolution was based on the MAEF source waveform data shown in Fig. 2 (right panel) and the simulated summary NAPs (Fig. 5f).

channels covering the frequency range from 100 to 10 000 Hz. The medium spontaneous-rate fibre specified in Meddis (1988) was used for the hair-cell simulator. Uppenkamp et al. (2001) have argued that the transmission-line filterbank is preferable to a gammatone filterbank because the non-linearity in the transmission line, improves the simulation of the kind of temporal asymmetry observed in masking experiments with Schroeder phase waves (e.g. Smith et al., 1995; Kohlrausch and Sander, 1995; Oxenham and Dau, 2001a,b).

Fig. 5 shows the NAPs of the stimuli used in the present study. A summary of the simulated activity in the AN was computed by averaging across the channels of the NAP. These summary NAPs represent the aggregate spike-probability density functions (PDFs) for the AN, and there are substantial differences between the summary NAPs for the five stimulus conditions. The up-chirp PDF has the largest peak and a delay of about 10 ms, relative to the PDF of the click. The down-chirp PDF has the smallest peak and the greatest spread, reflecting the greater cochlear dispersion. The peak in the PDF of the fast up-chirp is close to that of the up-chirp; the PDF of the fast down-chirp rises faster and has a higher peak than the PDF of the down-chirp. The PDF of the click has the fastest rise, and it is narrower than the PDF of the two down-chirps.

3.2. Methods

The unit response estimation was calculated in two steps. In the first step, the deconvolution was performed on the data of subject M.K., which had an exceptionally high signal-to-noise ratio and a clear separation of the N19–P30–N40 components. In the second step, the same deconvolution was performed using the left- and right-grand-average data shown in Fig. 4. Tikhonov regularisation was applied (Tikhonov, 1963; Hansen, 1992) to achieve stable and smooth solutions for the inverse problem inherent in deconvolution. The extraction of an appropriate and objective regularisation parameter for each stimulus condition was based on the generalised cross-correlation (GCV) function. All computations were done in MATLAB 6 (The Mathworks, Inc.). The analysis tools for regularisation problems, including the GCV function to extract the optimal parameter, were provided by Hansen (1998).

3.3. Results

Fig. 6 shows the unit responses for the five stimuli derived from the source waveforms of subject M.K. The deconvolution revealed two striking facts: first, the five unit responses are very similar; second, the latencies of the unit responses are much more similar than those of the corresponding MAEFs. In all conditions, the N40m peak is larger than the N19m peak, which is not observed in the grand average data. Deconvolution based on the grand average of all 11 subjects for the left and right hemispheres gives similar results, as shown in Fig. 7. The unit responses are very similar and the latency of the N19m and P30m peak vary little across the five conditions.

3.4. Discussion

The morphology of the MAEFs evoked by clicks and chirps indicates that the MAEF preserves aspects of the spatial dispersion on the BM. We modelled the MAEF, assuming that the MEG response is the *linear* superposition of excitation across frequency channels in the auditory pathway. The spike probability functions elicited by clicks and chirps in the AN were simulated with

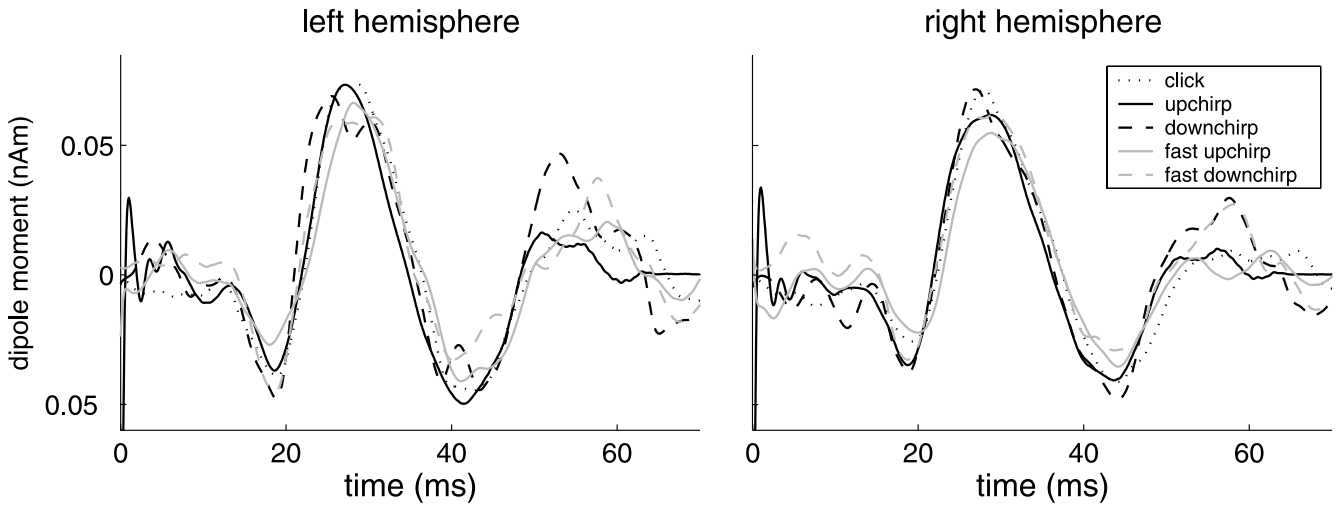

Fig. 7. Deconvolution of the grand average MAEF of the left and right auditory cortex. The unit responses derived from the five stimulus conditions are similar in both hemispheres.

the AIM using the transmission-line filterbank of Giguère and Woodland (1994). As expected, the summary NAPs exhibited large morphological differences. The up-chirp produced the summary NAP with the largest peak and the greatest shift (10 ms). The down-chirp produced the smallest peak and the greatest spread of activation in time.

The unit response (kernel) for each stimulus condition was derived by deconvolving the empirical MAEF response with the corresponding PDF.

The high similarity of the unit responses deconvolved from the far field recordings at the cortical level as measured by MEG with the NAPs of peripheral activation in conjunction with the fact that the peak-to-peak distances of the N19m–P30m complex differed significantly between the optimal up-chirp ($\alpha = 3.0$) and its time reversal (Fig. 3) provides evidence that the degree of peripheral synchronisation is passed on linearly from lower levels of the auditory pathway to higher sensory levels. Thus, since the cochleotopic organisation is maintained up to primary cortex and assuming no between-channel cancellation, the summary activation at each stage along the pathway is regarded as a convolution of the volley at the input of that certain stage and its specific electrophysiological within-channel unit response. At the level of the PAC such a unit response might reflect the neural activation of a narrow patch along the medio-lateral tonotopic axis of Heschl's gyrus

The value of deconvolution has also been demonstrated using steady-state responses by Schneider (2001). He observed an increase in MAEF latency when the frequency of a sinusoid is reduced from 5600 Hz to 100 Hz. Fig. 8 shows an overlay of (i) the MAEF responses evoked by sinusoids with frequencies ranging from 100 Hz to 5600 Hz, and (ii) the propagation time from de Boer's (1980) linear cochlear model. The third line shows the latency of ABR wave V derived with high-pass masking noise (Don and Eggermont, 1978). These curves show remarkable similarity; that is, the delay of wave V which represents activation in the midbrain, and the delay in PAC, follow a similar exponential decay. The structures appear to exhibit similar sensitivity to the spatial dispersion in the cochlea.

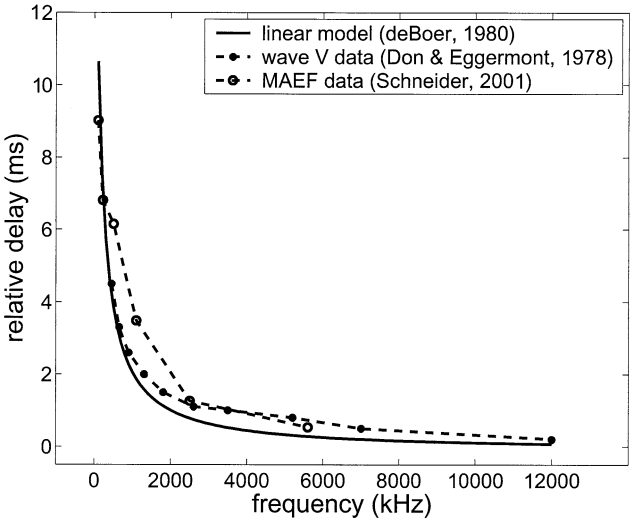

Fig. 8. Relative latency of ABR wave V (dotted line) and MAEF P30m of left and right hemisphere source waveforms (dashed line) as a function of centre frequency (MEG-data provided by Peter Schneider, Heidelberg, Germany). The ABR data are adapted from Don and Eggermont's (1978, p. 1088, Fig. 5) centre frequency plots. The solid line shows the latency calculated from the linear cochlear model of de Boer (1980). Curves were aligned along the time axis to illustrate the correspondence of the delay lines.

4. Summary and conclusions

Spatio-temporal source analysis was employed to describe activation in PAC, as recorded by MAEF, in response to short chirp stimuli with differing instantaneous frequency trajectories. The results support the observations reported by Scherg and Volk (1983) and Scherg and von Cramon (1990), that phase differences established in the cochlea between frequency channels propogate up through the brainstem and midbrain to PAC. This indicates the presence of a fast route from the cochlea to PAC that by-passes any temporal integration process which might exist in other pre-cortical processing modules (Wiegrebe and Winter, 2001; Griffiths et al., 2001). This interpretation is supported by the similarity of the unit responses obtained by deconvolution from the five stimulus conditions, and it indicates that the transient activation in PAC simply emerges as the superposition of activation across all frequency channels of the auditory pathway. This behaviour of the MAEF is in contrast to the behaviour of the late auditory N1–P2 complex as observed by Wegner et al. (1999) who recorded potential amplitudes evoked by the reversed chirp of the same size as evoked by the optimal chirp. Thus, at the level of the N100, neural activity appears to be integrated across frequency since the degree of synchronisation has much less effect on the amplitude of this component.

However the findings of the present paper raise the question as to the relationship between activation in PAC and perception. A recent psychoacoustical study on the perception of similar chirps (Uppenkamp et al., 2001) revealed that the difference in sound quality between up-chirps and down-chirps is different in form from the difference in the brainstem responses to these sounds (Dau et al., 2000) – a difference which the current study indicates is preserved in transient responses in PAC. Despite the increase in neural synchrony produced by up-chirps, and the decrease in neural synchrony produced by down-chirps, it is nevertheless the down-chirp that is perceived as the more compact event in time.

Uppenkamp et al. (2001) interpreted their results within the framework of the AIM. The first two stages in their simulation were essentially the same as in this study, that is, a non-linear transmission line simulation of BMM, and a hair-cell simulation of neural transduction (Meddis, 1988) to produce a NAP of spike probabilities. It appears that the summary NAP can largely account for the effects of chirp direction (and duration) on evoked activity in the brainstem (Dau et al., 2000) and PAC (the current study). Nevertheless, it appears that phase delays between channels, that affect the shape of the summary NAP and the MAEF, do not have a major effect on the sound quality of these clicks and chirps.

Uppenkamp et al. (2001) explain the discrepancy between the physiology and perception by pointing out that chirp direction has a second effect on the NAP; the impulse responses of the individual channels of the BMM and the NAP are more concentrated in time for clicks and down-chirps than for up-chirps (Uppenkamp et al., 2001, fig. 1). They conclude that this temporal fine structure within auditory channels is crucial for sound quality, while between-channel phase differences are largely removed by an additional process (time interval extraction) which is used to convert the NAP into the representation that we hear. They point out that the 'strobed' temporal integration mechanism in AIM would be one possible mechanism of time-interval extraction.

Using functional MRI, Griffiths et al. (2001) found evidence that this kind of process occurs before PAC, with some evidence that it may begin as early as the cochlear nucleus. The MAEFs recorded in the present study show that there is nevertheless a 'fast' route in the auditory pathway from cochlea to cortex that largely preserves phase differences between different frequency channels.

More evidence for the existence of at least two different processes is given by several empirical observations. First, Scherg and Volk (1983) showed that the latency difference between a 500 Hz tone and a click is reduced when the level of presentation is increased from 20 to 70 dB HL. This effect is probably due to upward spread of excitation in the cochlea. Similar observations have been reported by Dau et al. (2000). The 10-ms shift of the ABR response elicited by optimal up-chirp stimulation was reduced when the level reached 60 dB HL.

In summary, at this point we are still left with the contrast between physiological and perceptual data. While the *between-channel* phase alignment produced by synchronising up-chirps enhance wave V (Dau et al., 2000) and middle-latency responses due to peripheral synchronisation of tonotopic channels, the perceived compactness of up-chirps is reduced because the phase alignment also causes an enhancement of ringing *within* auditory channels for these up-chirps.

Acknowledgements

Research supported by the DFG (ZIZAS, grants SCHE-558/2-2 and Ru-652/1-3) and the UK Medical Research Council (G990369). Thanks to Peter Schneider for providing pure-tone MAEF data. The MRI data were provided by the Department of Neuroradiology, University of Heidelberg.

References

Ahonen, A.I., Hämäläinen, M.S., Kajola, M.J., Knuutila, J.E.T., Laine, P.P., Lounasmaa, O.V., Parkkonen, L.T., Simola, J.T., Tesche, C.D., 1993. 122-channel SQUID instrument for investigating the magnetic signals from the human brain. Phys. Scr. T49, 198–205.

de Boer, E., 1980. Auditory physics. Physical principles in hearing theory I. Phys. Rep. 62, 87–174.

Dau, T., Wegner, O., Mellert, V., Kollmeier, B., 2000. Auditory brainstem responses (ABR) with optimized chirp signals compensating basilar membrane dispersion. J. Acoust. Soc. Am. 107, 1530–1540.

Don, M., Eggermont, J.J., 1978. Analysis of click-evoked brainstem potentials in man using high-pass noise masking. J. Acoust. Soc. Am. 63, 1084–1092.

Giguère, C., Woodland, P.C., 1994. A computational model of the auditory periphery for speech and hearing research I, ascending path. J. Acoust. Soc. Am. 95, 331–342.

Griffiths, T.D., Uppenkamp, S., Johnsrude, I., Josephs, O., Patterson, R.D., 2001. Encoding of the temporal regularity of sound in the human brainstem. Nat. Neurosci. 4, 633–637.

Gutschalk, A., Mase, R., Roth, R., Ille, N., Rupp, A., Hähnel, S., Picton, T.W., Scherg, M., 1999. Deconvolution of 40 Hz steady-state fields reveals two overlapping source activities of the human auditory cortex. Clin. Neurophysiol. 110, 856–868.

Hansen, P.C.H., 1992. Rank-Deficient and Discrete Ill-Posed Problems. Numerical Aspects of Linear Inversion. SIAM, Philadelphia, PA.

Hansen, P.C.H., 1998. Regularisation tools. A Matlab package for analysis and solution of discrete ill-posed problems. http://www.imm.dtu.dk/~pch

Holm, S., 1979. A simple sequentially rejective multiple test procedure. Scand. J. Stat. 6, 65–70.

Kohlrausch, A., Sander, A., 1995. Phase effects in masking related to dispersion in the inner ear. II. Masking period matterns of short targets. J. Acoust. Soc. Am. 97, 1817–1829.

Liègeois-Chauvel, C., Musolino, A., Badier, J.M., Marquis, P., Chauvel, P., 1994. Evoked potentials recorded from the auditory cortex in man: evaluation and topography of the middle latency components. Electroencephalogr. Clin. Neurophysiol. 92, 204–214.

Meddis, R., 1988. Simulation of auditory-neural transduction: further studies. J. Acoust. Soc. Am. 83, 1056–1063.

Oxenham, A., Dau, T., 2001a. 'Reconciling frequency selectivity and phase effects in masking'. J. Acoust. Soc. Am. 110, 1525–1538.

Oxenham, A., Dau, T., 2001b. 'Towards a measure of auditory-filter phase response'. J. Acoust. Soc. Am. 110, 3169–3178.

Patterson, R.D., Robinson, K., Holdsworth, J., McKeown, D., Zhang, C., Allerhand, M., 1992. Complex sounds and auditory images. In: Cazals, Y., Demany, L., Horner, K. (Eds.), Auditory Physiology and Perception. Pergamon, Oxford, pp. 429–446.

Patterson, R.D., Allerhand, M.H., Giguère, C., 1995. Time-domain modelling of peripheral auditory processing: a modular architecture and a software platform. J. Acoust. Soc. Am. 98, 1890–1894.

Rupp, A., Hack, S., Gutschalk, A., Schneider, P., Picton, T.W., Scherg, M., 2000. Fast temporal interactions in human auditory cortex. NeuroReport 11, 3731–3736.

Scherg, M., Volk, S.A., 1983. Frequency specificity of simultaneously recorded early and middle latency auditory evoked potentials. Electroencephalogr. Clin. Neurophysiol. 56, 443–452.

Scherg, M., von Cramon, D., 1990. Dipole source potentials of the auditory cortex in normal subjects and in patients with temporal lobe lesions. In: Hoke, M. (Ed.), Advances in Audiology. Karger, Basel, pp. 165–192.

Scherg, M., Hari, R., Hämäläinen, M., 1989. Frequency-specific sources of the auditory N19-P30-P50 response detected by a multiple source analysis of evoked magnetic fields and potentials. In: Williamson, S.J., Hoke, M., Sroink, G. (Eds.), Advances in Biomagnetis. Plenum Press, New York, pp. 97–100.

Schneider, P., 2001. Source Activity and Tonotopic Organization of the Auditory Cortex in Musicians and Non-Musicians. PhD Thesis. University of Heidelberg.

Shore, S.E., Nuttall, A.L., 1985. High-synchrony cochlear compound action potentials evoked by rising frequency-swept tone bursts. J. Acoust. Soc. Am. 78, 1286–1295.

Shore, S.E., Clopton, B.M., Yolande, N., 1987. Unit responses in ventral cochlear nucleus reflect cochlear coding of rapid frequency sweeps. J. Acoust. Soc. Am. 82, 471–478.

Sprent, P., Smeeton, N.C. (2001). Applied Nonparametric Statistical Methods. 3rd edn. Chapman and Hall, Boca Raton, FL.

Tikhonov, A.N., 1963. Solution of incorrectly formulated problems and the regularization method. Sov. Math. Dokl. 4, 1035–1038.

Uppenkamp, S., Fobel, S., Patterson, R.D., 2001. The effects of temporal asymmetry on the detection and perception of short chirps. Hear. Res. 158, 71–83.

von Békésy, G., 1960. Experiments in Hearing. McGraw-Hill, New York.

Webster, D.E., 1992. An overview of mammalian pathways with an emphasis on humans. In: Webster, D.E., Popper, A.N., Fay, R.R. (Eds.). The Mammalian Pathway: Neuroanatomy. Springer, New York, pp. 1–22.

Wegner, O., Dau, T., 2002. Frequency specificity of chirp-evoked auditory brainstem responses. J. Acoust. Soc. Am. 111, 1318–1329.

Wegner, O., Dau, T., Kollmeier, B., 1999. On the relationship between auditory evoked potentials and psychophysical loudness. In: Dau, T., Hohmann, V., Kollmeier, B. (Eds.), Psychophysics, Physiology and Models of Hearing. World Scientific, Singapore, pp. 59–62.

Wiegrebe, L., Winter, I.M., 2001. Temporal representation of iterated rippled noise as a function of delay and sound level in the ventral cochlear nucleus. J. Neurophysiol. 85, 1206–1219.